Activation cross sections of alpha-particle induced nuclear reactions on natural palladium

M. Aikawa[a,*], M. Saito[b,1], Y. Komori[c], H. Haba[c], S. Takács[d], F. Ditrói[d], Z. Szűcs[d]

[a] Faculty of Science, Hokkaido University, Sapporo 060-0810, Japan

[b] Graduate School of Science, Hokkaido University, Sapporo 060-0810, Japan

[c] Nishina Center for Accelerator-Based Science, RIKEN, Wako 351-0198, Japan

[d] Institute for Nuclear Research, Hungarian Academy of Sciences (ATOMKI), 4026 Debrecen, Hungary

Keyword

Excitation function; Cross section; Alpha-particle irradiation; Palladium target

Abstract

The activation cross sections of the alpha-particle induced reactions on natural palladium were determined up to 50 MeV using the stacked-foil technique and high-resolution gamma-ray spectrometry. Production cross sections of ^{111m,109,107,105,104}Cd and ^{111g,110m,106m,105g,103g}Ag were obtained. The results were compared with the data of previous experiments and results of theoretical model calculations.

1. Introduction

Production cross sections of medical radioactive isotopes (RI) are fundamental information for applications such as therapy and diagnostics [1,2]. The knowledge on the cross sections is required to optimize the production of a radioisotope and to produce the appropriate amount of RI. One of such medical RI is the ^{103}Pd ($T_{1/2}$ = 16.991 d), which is used for brachytherapy [3,4] and targeted radionuclide therapy as part of the ^{103}Pd/^{103m}Rh *in vivo* generator [5]. In addition to the direct production of ^{103}Pd, it is worth to investigate the production of its parent, ^{103}Ag. The ^{103}Ag has an isomeric state ^{103m}Ag at 134.4 keV excitation energy ($T_{1/2}$ = 5.7 s), which cumulatively contributes to the production of the ground state ^{103g}Ag ($T_{1/2}$ = 65.7 min).

* Corresponding author: aikawa@sci.sci.hokudai.ac.jp

[1] Present address: Graduate School of Biomedical Science and Engineering, Hokkaido University, Sapporo 060-8638, Japan

Several charged-particle induced reactions on ^{nat}Pd can be considered for the ^{103}Ag production. According to the survey in the EXFOR library [6], proton- [4,7–9], deuteron- [4,10,11] , ^{3}He- [12] and alpha-induced reactions [13] on ^{nat}Pd already have been studied. In the case of alpha-particle induced reactions on ^{nat}Pd, only one experimental dataset is available below 37 MeV [13]. Therefore, we are motivated to perform an experiment to determine the excitation function of the ^{nat}Pd(α,x)^{103}Ag reaction at higher energy. In addition to the ^{103g}Ag production, we also deduced activation cross sections of several Cd and Ag isotopes, ^{111m,109,107,105,104}Cd and ^{111g,110m,106m,105g}Ag, in our experiment up to 50 MeV.

2. Experimental

The experiment was performed at the RIKEN AVF cyclotron by using the standard stacked-foil technique and the activation method with high-resolution gamma-ray spectrometry. Thin palladium foils (purity 99.95%, Nilaco Corp., Japan) with natural isotopic composition (^{102}Pd 1.02%, ^{104}Pd 11.14%, ^{105}Pd 22.33%, ^{106}Pd 27.33%, ^{108}Pd 26.46%, ^{110}Pd 11.72%) were used with ^{nat}Ti monitor foils (purity 99.9%, Goodfellow Co., Ltd., UK). The foils were cut from a larger sheet, of which size and weight were measured. Average thicknesses of the Pd and Ti foils were found to be 9.70 mg/cm^2 and 4.85 mg/cm^2, respectively. The stacked target consisted of 12 sets of the group of Pd-Pd-Ti-Ti foils. Foils were doubled to compensate the recoil effect in every second foil at the downstream of the beam. The stacked foil target was irradiated for 2 hours by the 51.2 ± 0.1 MeV alpha-particle beam with an average intensity of 111.4 nA, which was measured by a Faraday cup. The initial beam energy was determined by the time-of-flight method using a plastic scintillator monitor [14]. The energy degradation of the beam in the stack was calculated using the polynomial approximation of the stopping power data [15]. The γ-spectra of the irradiated foils were measured by HPGe detectors (ORTEC GEM-25185-P and ORTEC GEM35P4-70) and analyzed by Gamma Studio (SEIKO EG&G). To follow the decay of the reaction products with half-lives between 50 min. and 460 days spectra were measured four times. The cooling times of the measurements are 45 min, 3.6 hours, 2.3 and 244 days, respectively. Nuclear decay data were taken from the online NuDat 2.7 database [16] and Q-value calculator [17] (Table 1).

Table 1
Reaction and decay data of the investigated reaction products. Only the gamma-lines used in the analysis are listed

Reaction product	Half-life	Decay mode (%)	E_γ (keV)	I_γ (%)	Contributing reactions	Q-value (MeV)
^{111m}Cd	48.54 min	IT (100)	245.395	94(7)	^{108}Pd(α,n)	-5.9
					^{110}Pd(α,3n)	-20.9
^{109}Cd	461.4 d	ε (100)	88.0336	3.644(16)	^{105}Pd(α,γ)	2.5
					^{106}Pd(α,n)	-7.0
					^{108}Pd(α,3n)	-22.8
					^{110}Pd(α,5n)	-37.8
^{107}Cd	6.50 h	ε (100)	93.124	4.7(3)	^{104}Pd(α,n)	-8.1
					^{105}Pd(α,2n)	-15.1
					^{106}Pd(α,3n)	-24.7

					^{108}Pd(α,5n)	-40.5
^{105}Cd	55.5 min	ε (100)	961.84	4.7(3)	^{102}Pd(α,n)	-9.2
			346.87	4.2(3)	^{104}Pd(α,3n)	-26.9
					^{105}Pd(α,4n)	-33.9
					^{106}Pd(α,5n)	-43.5
^{104}Cd	57.7 min	ε (100)	709.3	19.5(24)	^{102}Pd(α,2n)	-17.7
					^{104}Pd(α,4n)	-35.3
					^{105}Pd(α,5n)	-42.4
^{111g}Ag	7.45 d	β^- (100)	342.13	6.7	^{108}Pd(α,p)	-6.2
					^{110}Pd(α,t)	-12.6
					^{110}Pd(α,αn)^{111}Pd(β^-) decay	-8.8
^{110m}Ag	249.83 d	β^- (98.67)	657.7600	95.61	^{108}Pd(α,d)	-12.8
		IT (1.33)	884.6781	75.0(11)	^{110}Pd(α,tn)	-21.5
^{106m}Ag	8.28 d	ε (100)	450.976	28.2(7)	^{104}Pd(α,d)	-13.2
					^{105}Pd(α,t)	-14.0
					^{106}Pd(α,tn)	-23.6
					^{108}Pd(α,t3n)	-39.3
^{105g}Ag	41.29 d	ε (100)	344.52	41.4	^{102}Pd(α,p)	-5.7
					^{104}Pd(α,t)	-14.8
					^{105}Pd(α,tn)	-21.9
					^{106}Pd(α,t2n)	-31.5
					^{108}Pd(α,t4n)	-47.3
					^{105}Cd(ε) decay	
^{103g}Ag	65.7 min	ε (100)	118.74	31.2(20)	^{102}Pd(α,t)	-15.6
					^{104}Pd(α,t2n)	-33.3
					^{105}Pd(α,t3n)	-40.4
					^{106}Pd(α,t4n)	-49.9
					^{103}Cd(ε) decay	

The excitation function of the ^{nat}Ti(α,x)^{51}Cr monitor reaction was derived from the decay of the ^{51}Cr ($T_{1/2}$ = 27.7025 d) isotope by measuring the activity of its γ-line at 320.0824 keV (I_γ = 9.910%). The result is shown in Fig. 1 in comparison with the recommended value [18]. An agreement within the experimental uncertainty was found, which confirms the beam intensity measurement and the energy scale calculation throughout the stack.

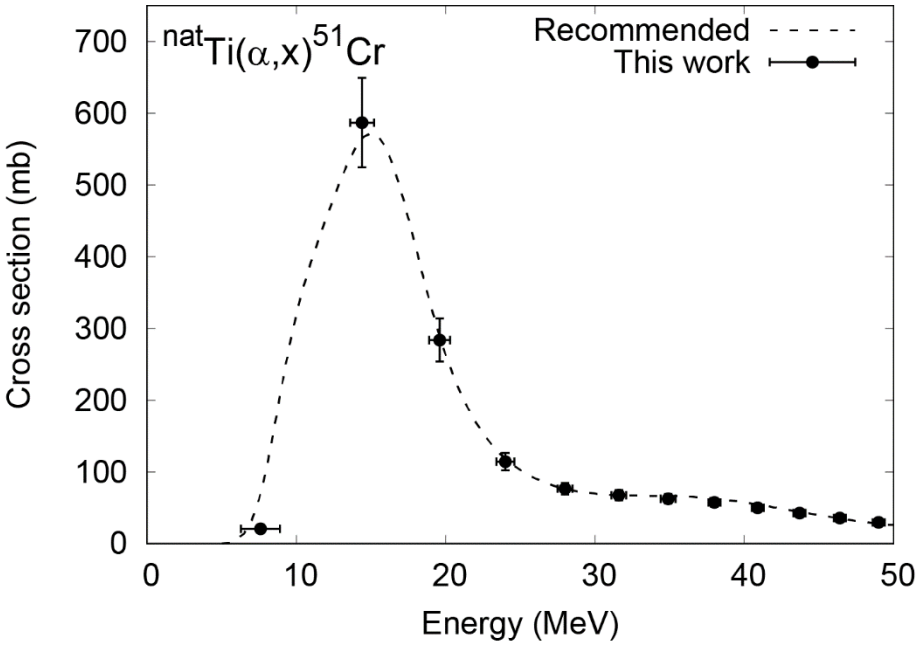

Fig. 1. Comparison of the recommended excitation function of the $^{nat}Ti(\alpha,x)^{51}Cr$ monitor reaction with the experimental cross section values.

3. Result and Discussion

The production cross sections of Cd and Ag isotopes for alpha-particle induced reactions on ^{nat}Pd determined in this work are summarized in Tables 2 and 3. The results graphically shown in Figs. 2-11 are compared with previous experimental data [13] and result of TALYS model calculation taken from TENDL-2017 online database [19]. The individual cross sections listed in TENDL-2017 database are multiplied by abundance of the corresponding Pd isotopes and summed up to be able to compare with the experimental data.

The total uncertainty was estimated to be 10.6-37.0 % including statistical errors (0.1-34.8%). It was derived from the square root of the quadratic summation of the components; the beam intensity (7%), target thickness (2%), target purity (1%), detector efficiency (7%), gamma intensity (<7%) and peak area determination (3%).

Table 2

Production cross sections of Cd isotopes.

Energy (MeV)	^{111m}Cd (mb)	^{109}Cd (mb)	^{107}Cd (mb)	^{105}Cd (mb)	^{104}Cd (mb)
50.1 ±0.5	21.9 ±2.9	100.2 ±11.4	120.0 ±14.8	75.8 ±11.0	20.1 ±3.6
47.6 ±0.5	28.0 ±3.7	107.6 ±11.9	147.6 ±18.3	71.4 ±10.3	13.0 ±2.4
44.9 ±0.5	38.1 ±4.9	137.8 ±15.0	192.4 ±23.8	63.1 ±8.3	6.8 ±1.3
42.2 ±0.5	67.4 ±8.7	231.3 ±24.9	294.2 ±36.4	67.7 ±8.7	3.7 ±0.8
39.3 ±0.6	98.5 ±12.8	319.7 ±34.2	333.3 ±41.2	50.2 ±6.3	2.6 ±0.5
36.3 ±0.6	135.0 ±17.5	354.6 ±37.9	360.0 ±44.5	40.2 ±5.5	4.3 ±0.9
33.1 ±0.6	138.7 ±18.0	322.2 ±34.4	357.6 ±44.2	10.1 ±3.7	6.5 ±1.6
29.6 ±0.7	101.2 ±13.2	181.7 ±19.6	309.9 ±38.3		7.8 ±2.2
25.9 ±0.7	39.7 ±5.3	32.6 ±3.8	296.1 ±36.6		7.5 ±2.2
21.7 ±0.8	20.4 ±2.9	63.3 ±7.0	244.3 ±30.2		
17.0 ±1.0	44.6 ±6.2	115.1 ±12.2	55.9 ±6.9		
11.1 ±1.2			0.25 ±0.03		

Table 3

Production cross sections of Ag isotopes.

Energy (MeV)	^{111g}Ag (mb)	^{110m}Ag (mb)	^{106m}Ag (mb)	^{105g}Ag (mb)	^{103g}Ag (mb)
50.1 ±0.5	14.4 ±1.7	10.7 ±1.2	80.3 ±8.7	242.2 ±26.3	6.5 ±0.9
47.6 ±0.5	15.4 ±1.8	9.4 ±1.0	74.8 ±8.1	220.3 ±23.9	7.6 ±1.0
44.9 ±0.5	14.2 ±1.6	8.1 ±0.9	68.1 ±7.4	190.4 ±20.7	8.1 ±1.0
42.2 ±0.5	16.8 ±2.0	9.1 ±1.0	76.3 ±8.3	186.1 ±20.2	9.2 ±1.2

39.3 ±0.6	14.3 ±1.7	9.3 ±1.0	65.6 ±7.1	142.0 ±15.4	7.6 ±0.9
36.3 ±0.6	10.9 ±1.2	10.0 ±1.1	52.2 ±5.7	98.8 ±10.7	4.7 ±0.6
33.1 ±0.6	7.6 ±0.9	10.4 ±1.1	35.6 ±3.9	42.7 ±4.6	1.1 ±0.4
29.6 ±0.7	5.5 ±0.7	7.0 ±0.8	19.0 ±2.1	5.1 ±0.6	
25.9 ±0.7	5.0 ±0.6	2.8 ±0.3	8.1 ±0.9	3.8 ±0.4	
21.7 ±0.8	3.3 ±0.4	0.22 ±0.04	0.54 ±0.06	9.0 ±1.0	
17.0 ±1.0	0.33 ±0.04			4.7 ±0.5	
11.1 ±1.2	0.018 ±0.005			0.068 ±0.012	

3.1. The $^{nat}Pd(\alpha,x)^{111m}Cd$ Reaction

The excitation function of the $^{nat}Pd(\alpha,x)^{111m}Cd$ reaction was derived from the measurement of the γ-line at 245.395 keV (I_γ = 94%). The result is shown in Fig. 2 together with previous experimental data and TENDL-2017 data. The excitation function of this reaction has two wide peaks at around 15 and 35 MeV, corresponding to contributions of two stable isotopes of palladium, ^{108}Pd and ^{110}Pd. Our data are in general agreement with the earlier published data. However, the amplitude of our result is slightly larger than both the data published before as well as the result of TALYS calculation at around the peak at 35 MeV.

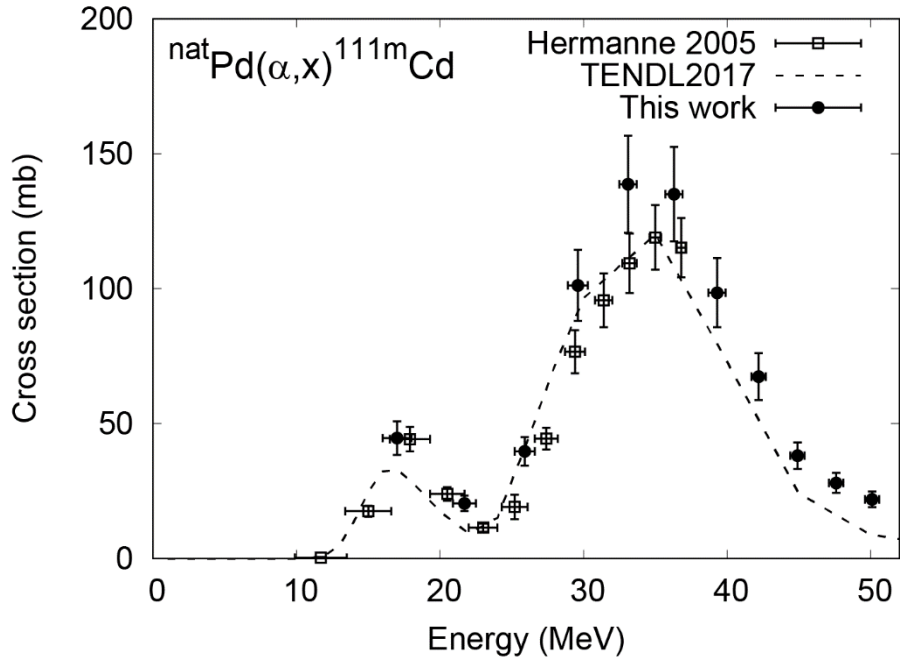

Fig. 2. The excitation function of the $^{nat}Pd(\alpha,x)^{111m}Cd$ reaction.

3.2. The $^{nat}Pd(\alpha,x)^{109}Cd$ Reaction

The γ-line at 88.0336 keV (I_γ = 3.644%) from the decay of ^{109}Cd ($T_{1/2}$ = 461.4 d) was measured after a long cooling time (244 days) to reduce the effect of other coproduced radioisotopes. The excitation function of the $^{nat}Pd(\alpha,x)^{109}Cd$ reaction is shown in Fig. 3 in comparison with TENDL-2017 data. The result has two peaks at around 15 and 35 MeV, corresponding to the dominant contribution of the reactions on the ^{106}Pd and ^{108}Pd target isotopes. It has a similar shape with but different amplitudes from that of the $^{nat}Pd(\alpha,x)^{111m}Cd$ reaction. No earlier experimental data are available for this reaction. Our result shows slightly larger values, however the behavior is consistent with data of TENDL-2017 database.

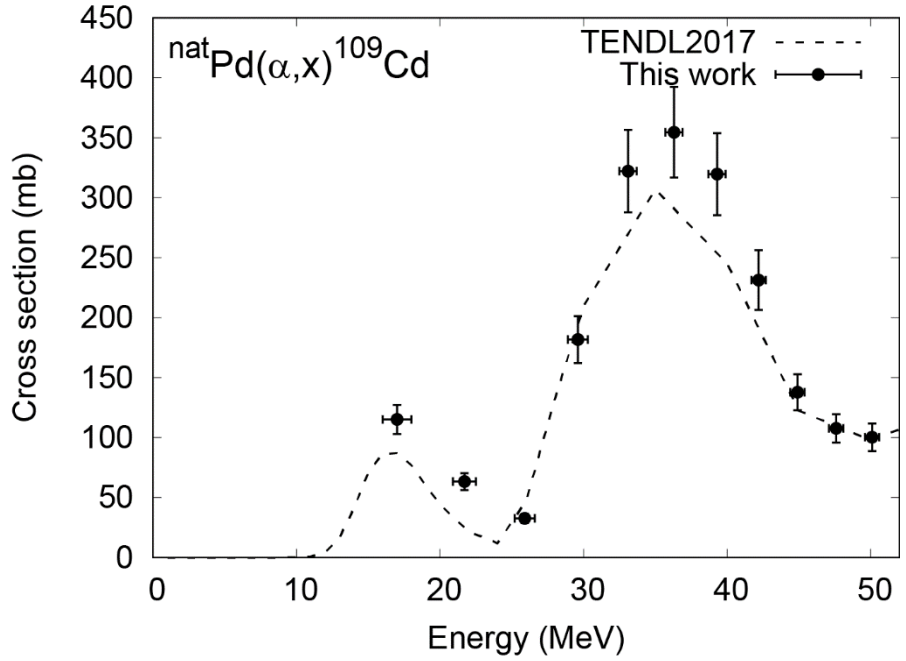

Fig. 3. The excitation function of the $^{nat}Pd(\alpha,x)^{109}Cd$ reaction.

3.3. The $^{nat}Pd(\alpha,x)^{107}Cd$ Reaction

The production cross sections of ^{107}Cd ($T_{1/2}$ = 6.50 h) were measured using the independent γ-line at 93.124 keV (I_γ = 4.7%). The result is shown in Fig. 4 together with data from TENDL-2017 database. There are three contributing reactions, the $^{104}Pd(\alpha,n)$, $^{105}Pd(\alpha,2n)$ and $^{106}Pd(\alpha,3n)$ reactions, which compose one broad peak at around 35 MeV. The shape is different from those of the $^{nat}Pd(\alpha,x)^{109,111m}Cd$ reactions having two independent peaks dominated by two contributing reactions. The result of TALYS calculation represents relatively well our experimental data.

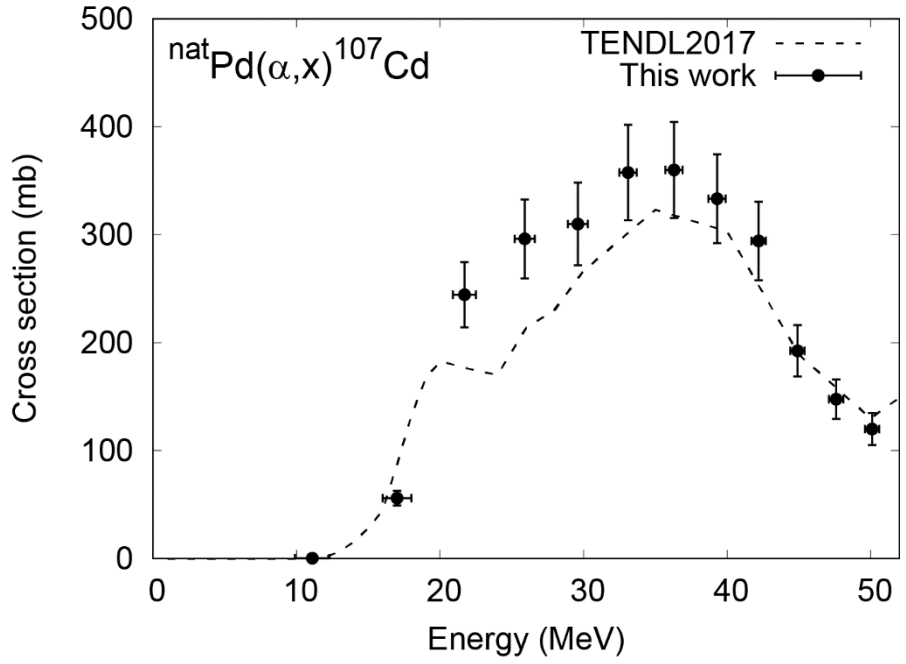

Fig. 4. The excitation function of the $^{nat}Pd(\alpha,x)^{107}Cd$ reaction.

3.4. The $^{nat}Pd(\alpha,x)^{105}Cd$ Reaction

The γ-line at 961.84 keV (I_γ = 4.7%) from the decay of ^{105}Cd ($T_{1/2}$ = 55.4 min) was assessed for determining the excitation function of the $^{nat}Pd(\alpha,x)^{105}Cd$ process. This γ-line has a negligible interference with the 962.43 keV γ-line (I_γ = 0.124%) from the decay of much longer-lived ^{105}Ag coproduced isotope ($T_{1/2}$ = 41.29 d). The measurement was performed after a cooling time of 3.6 hours. The derived result is shown in Fig. 5 in comparison with earlier experimental data and result of theoretical estimation taken from TENDL-2017 database. The earlier data are slightly higher than our data and the theoretical calculation is overestimate both of the experimental data sets above 30 MeV.

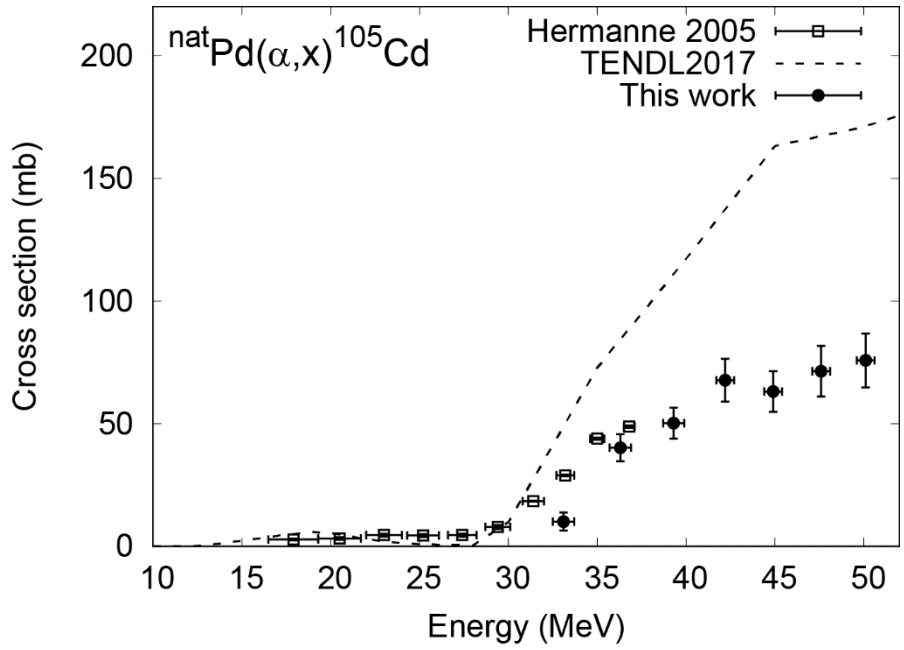

Fig. 5. The excitation function of the $^{nat}Pd(\alpha,x)^{105}Cd$ reaction.

3.5. The $^{nat}Pd(\alpha,x)^{104}Cd$ Reaction

The γ-line at 709.3 keV (I_γ = 19.5%) from the decay of ^{104}Cd ($T_{1/2}$ = 57.7 min) was used for determination the excitation function of the $^{nat}Pd(\alpha,x)^{104}Cd$ reaction. There are small overlapped contributions to the total peak area from decay of ^{105}Cd and ^{111}Pd. The contribution of 709.87 keV γ-line (I_γ = 0.127%) from the ^{105}Cd decay was subtracted using the cross sections obtained in section 3.4. The 709.8 keV γ-line (I_γ = 0.131%) from the ^{111}Pd decay was negligible because the γ-line at 172.18 keV (I_γ = 46%) could not be found. The more intense γ-line at 83.5 keV (I_γ = 47%) has a strong contribution from decay of ^{100}Pd and therefore unselected. The result is shown in Fig. 6 with earlier experimental data and data from TENDL-2017 data library. The previous data are in good agreement with our data. The theoretical estimation also gives relatively not too bad description of the experimental data of this process.

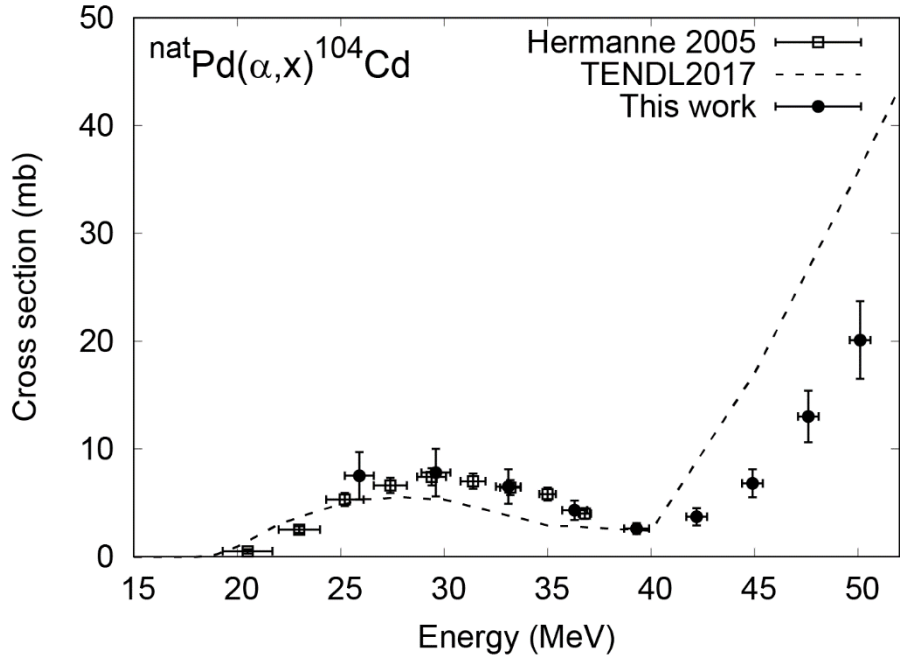

Fig. 6. The excitation function of the $^{nat}Pd(\alpha,x)^{104}Cd$ reaction.

3.6. The $^{nat}Pd(\alpha,x)^{111g}Ag$ Reaction

^{111}Ag has an excited isomeric state ^{111m}Ag ($T_{1/2}$ = 64.8 s) decaying almost completely to the ground state ^{111g}Ag ($T_{1/2}$ = 7.45 d) and contributes its population. Both isomeric states of ^{111}Pd, the ^{111g}Pd ($T_{1/2}$ = 23.4 min) and ^{111m}Pd ($T_{1/2}$ = 5.5 h), were produced in the $^{nat}Pd(\alpha,x)^{111}Pd$ process and contributed to the ^{111g}Ag production. The $^{nat}Pd(\alpha,x)^{111g}Ag$ reaction is thus cumulative one. The interference free γ-line at 342.13 keV (I_γ = 6.7%) from the decay of ^{111g}Ag has been measured after the cooling time of about 60 hours. The result is shown in Fig. 7 together with earlier published experimental data and prediction of TALYS calculation. Our results are in good agreement with previous experimental data. The theoretical calculation underestimates the experimental values, but provides an excitation function with a similar shape.

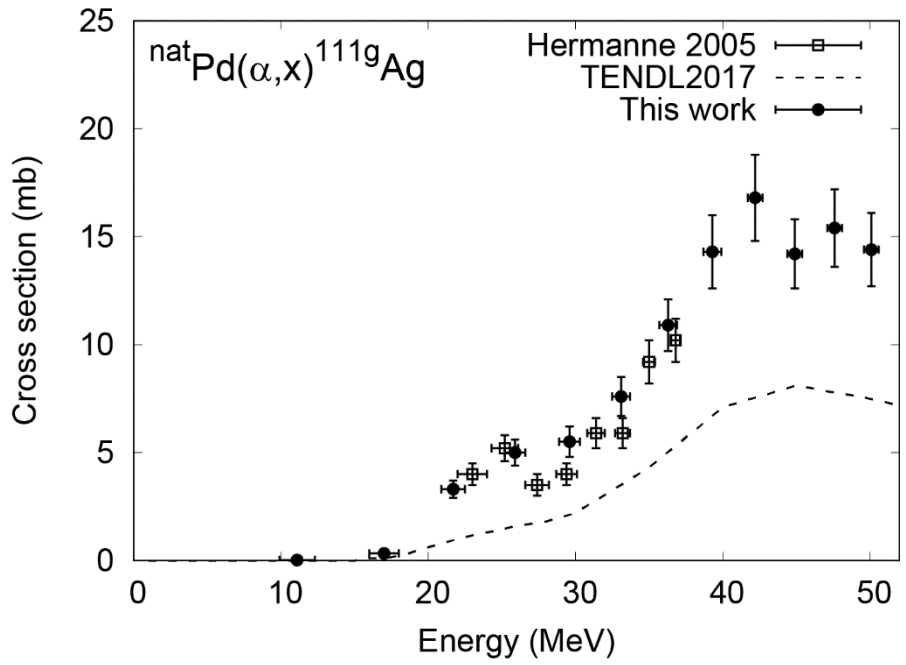

Fig. 7. The excitation function of the $^{nat}Pd(\alpha,x)^{111g}Ag$ reaction.

3.7. The $^{nat}Pd(\alpha,x)^{110m}Ag$ Reaction

The ^{110}Ag isotope has a short-lived ground state ($T_{1/2}$ = 24.5 s) and a much longer-lived excited isomeric state ^{110m}Ag ($T_{1/2}$ = 249.83 d). The interference free γ-line at 657.7600 keV (I_γ = 95.61%) from the decay of ^{110m}Ag has been used for determining the excitation function of the $^{nat}Pd(\alpha,x)^{110m}Ag$ reaction. The measurement was performed after a long cooling time of 244 days. Our results are shown in Fig. 8 together with the experimental data published earlier and results of theoretical calculation taken from TENDL-2017 database. The earlier measured data are in agreement with our result up to 30 MeV, but systematically higher above that energy. The theoretical calculation significantly underestimates this process.

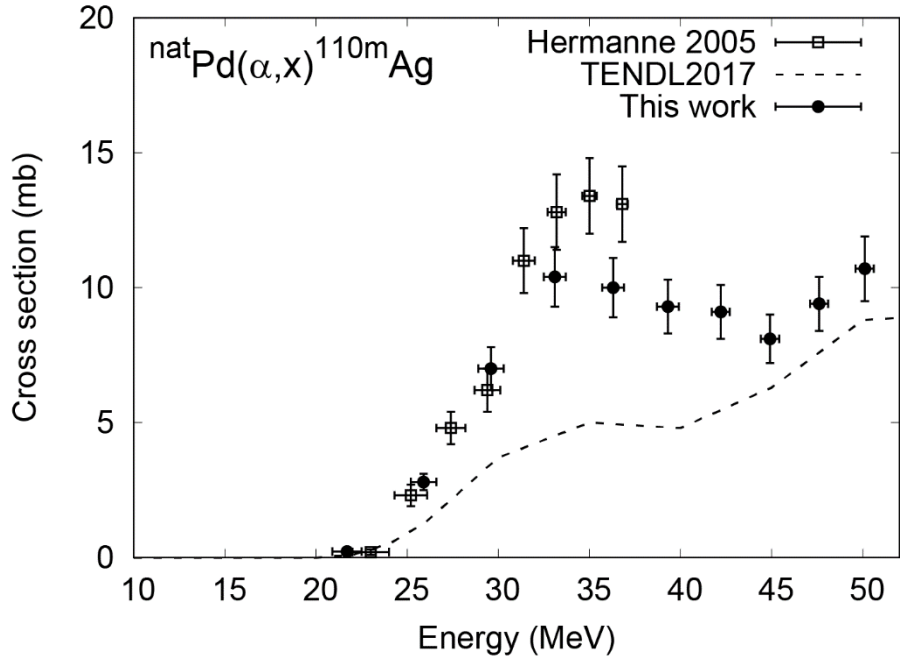

Fig. 8. The excitation function of the $^{nat}Pd(\alpha,x)^{110m}Ag$ reaction.

3.8. The $^{nat}Pd(\alpha,x)^{106m}Ag$ Reaction

The ^{106}Ag isotope has a short-lived ground state ^{106g}Ag ($T_{1/2}$ = 23.96 min) and a longer-lived isomeric state ^{106m}Ag ($T_{1/2}$ = 8.28 d). In this work only the higher energy isomeric state was assessed. The γ-line at 450.976 keV (I_γ = 28.2%) from the decay of ^{106m}Ag has been used to determine the cross section for this process after cooling time about 55 hours. This γ-line can be considered as independent after the applied cooling time when ^{106m}Rh ($T_{1/2}$ = 131 min) had completely decayed. The result is shown in Fig. 9 in comparison with the earlier experimental data and data taken from TENDL-2017 data library. The two experimental datasets are in good agreement with each other and the theoretical calculation also describes relatively well the experimental excitation function.

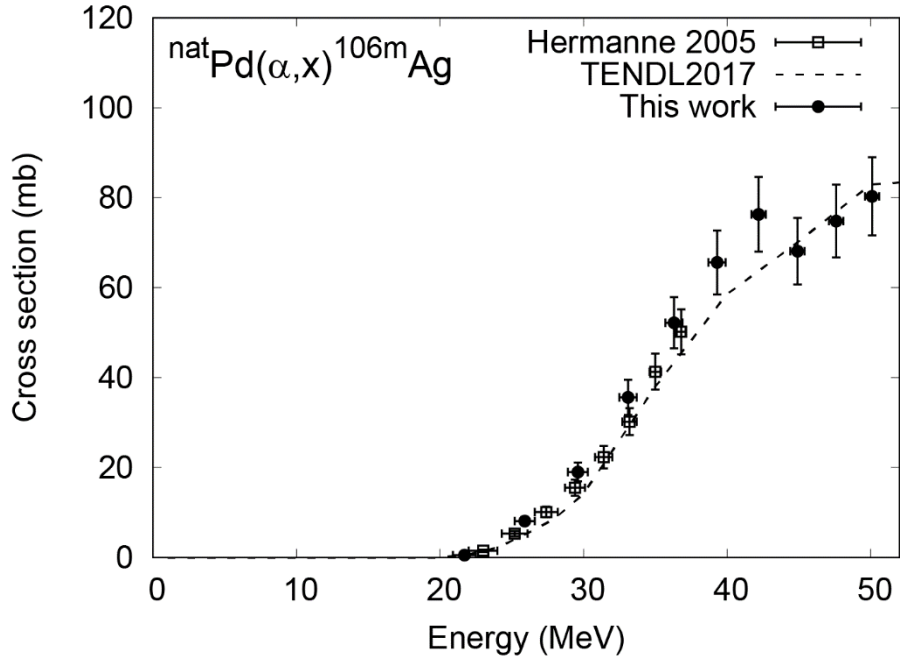

Fig. 9: The excitation function of the $^{nat}Pd(\alpha,x)^{106m}Ag$ reaction.

3.9. The $^{nat}Pd(\alpha,x)^{105g}Ag$ Reaction

The excitation function provided for the $^{nat}Pd(\alpha,x)^{105g}Ag$ reaction is cumulative since the decay of ^{105m}Ag ($T_{1/2}$ = 7.23 min) and ^{105}Cd ($T_{1/2}$ = 55.5 min) contribute to the formation of ^{105g}Ag. The γ-line at 344.52 keV (I_γ = 41.4%) from the decay of ^{105g}Ag ($T_{1/2}$ = 41.29 d) has been measured and is free from interferences after the long cooling time of about 60 days. The result is shown in Fig. 10 together with experimental data published earlier and result of TALYS model calculation taken from TENDL-2017 data library. Our result is in good agreement with the previous data and theoretical estimation also describes well this process, although the theoretical calculation overestimates the $^{nat}Pd(\alpha,x)^{105}Cd$ reaction which contributes to this process.

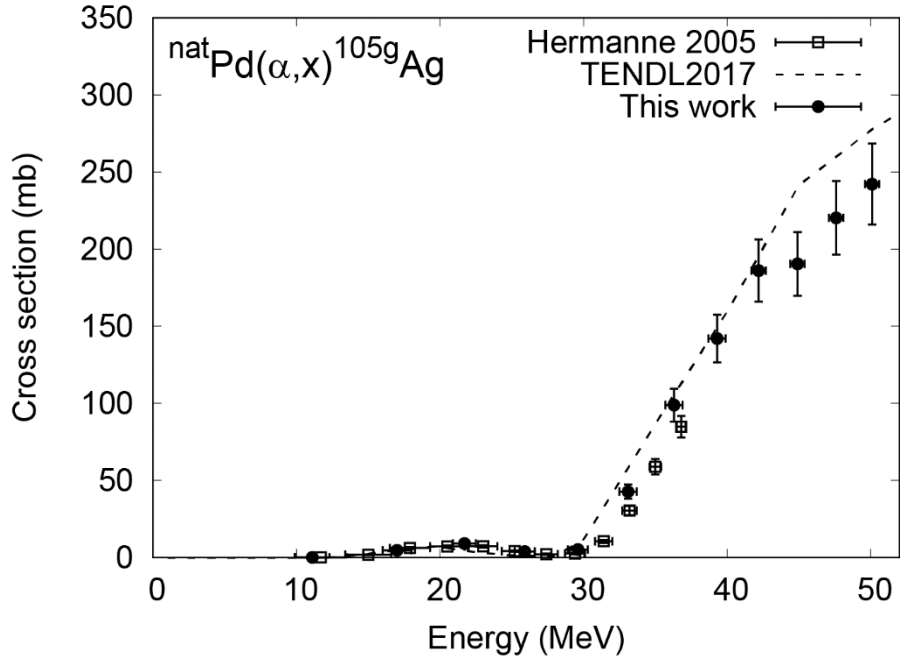

Fig. 10. The excitation function of the $^{nat}Pd(a,x)^{105g}Ag$ reaction.

3.10. The $^{nat}Pd(\alpha,x)^{103g}Ag$ Reaction

The γ-line at 118.74 keV (I_γ = 31.2%) from the decay of ^{103g}Ag ($T_{1/2}$ = 65.7 min) was measured after a cooling time of 3.6 hours and used to determine the excitation function of this process. Beside the direct production, ^{103g}Ag is populated by decay of its higher energy isomer state and by decay of ^{103}Cd ($T_{1/2}$ = 7.3 min), and therefore cumulative cross sections are deduced. There are minor contributions to this peak area from coproduced isotopes, but their total contribution is negligibly small. The result is shown in Fig. 11 in comparison with earlier experimental data and data from TENDL-2017 library. Our result is slightly higher than the previous experimental data. The TALYS calculation provides an excitation function with a consistent tendency.

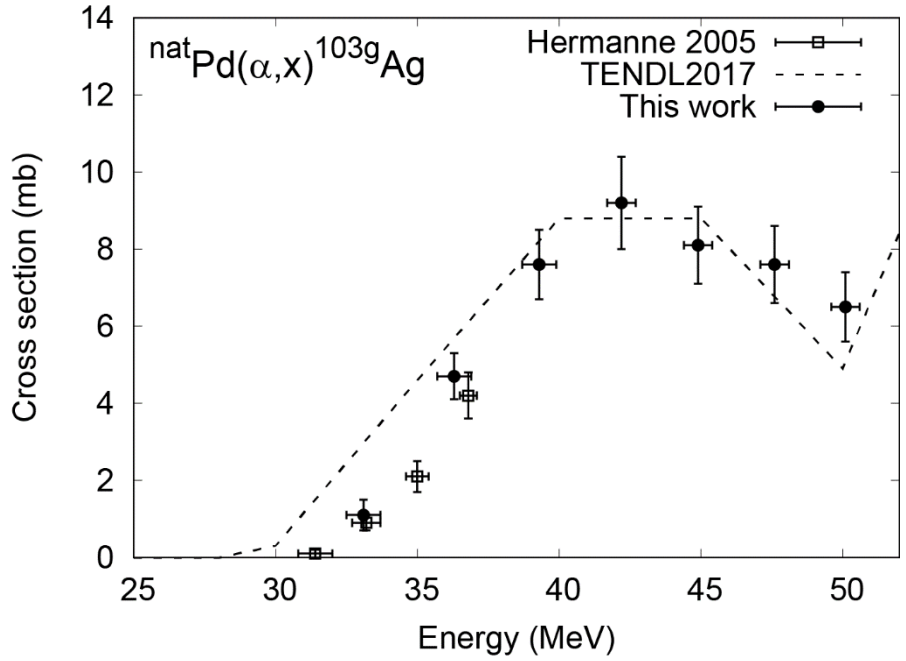

Fig. 11. The excitation function of the $^{nat}Pd(\alpha,x)^{103g}Ag$ reaction.

Conclusion

We have studied the alpha-particle induced nuclear reactions of palladium and derived activation cross section data for ^{111m,109,107,105,104}Cd and ^{111,110m,106m,105g,103g}Ag isotopes. The newly measured experimental cross sections were compared to the available earlier published data and in most cases agreement was found. The prediction of TALYS theoretical model calculation was also compared to the experimental data and acceptable agreement was found. The new data at the higher energy region up to 50 MeV enrich nuclear reaction databases and are available for improvement of theoretical model calculations.

Acknowledgement

The experiment was carried out at RI Beam Factory operated by RIKEN Nishina Center and CNS, University of Tokyo, Japan. This work is supported by the Japan - Hungary Research Cooperative Program, JSPS and HAS and by JSPS KAKENHI Grant Number 17K07004.

Reference

[1] F. Ditrói, F. Tárkányi, S. Takács, A. Hermanne, New developments in the experimental data for charged particle production of medical radioisotopes, J. Radioanal. Nucl. Chem. 305 (2015) 247–253. doi:10.1007/s10967-015-3968-x.

[2] S.M. Qaim, Nuclear data for production and medical application of radionuclides: Present status and future needs, Nucl. Med. Biol. 44 (2017) 31–49. doi:10.1016/j.nucmedbio.2016.08.016.

[3] S. Nag, D. Beyer, J. Friedland, P. Grimm, R. Nath, American brachytherapy society (ABS) recommendations for transperineal permanent brachytherapy of prostate cancer, Int. J. Radiat. Oncol. Biol. Phys. 44 (1999) 789–799. doi:10.1016/S0360-3016(99)00069-3.

[4] A. Hermanne, S. Takács, F. Tárkányi, R. Bolbos, Cross section measurements of proton and deuteron induced formation of ^{103}Ag in natural palladium, Radiochim. Acta. 92 (2004) 215–218. doi:10.1524/ract.92.4.215.35609.

[5] Z. Szucs, J. van Rooyen, J.R. Zeevaart, Recoil effect on β-decaying in vivo generators, interpreted for ^{103}Pd/^{103m}Rh, Appl. Radiat. Isot. 67 (2009) 1401–1404. doi:10.1016/j.apradiso.2009.02.022.

[6] N. Otuka, E. Dupont, V. Semkova, B. Pritychenko, A.I. Blokhin, M. Aikawa, S.

Babykina, M. Bossant, G. Chen, S. Dunaeva, R.A. Forrest, T. Fukahori, N. Furutachi, S. Ganesan, Z. Ge, O.O. Gritzay, M. Herman, S. Hlavač, K. Kato, B. Lalremruata, Y.O. Lee, A. Makinaga, K. Matsumoto, M. Mikhaylyukova, G. Pikulina, V.G. Pronyaev, A. Saxena, O. Schwerer, S.P. Simakov, N. Soppera, R. Suzuki, S. Takács, X. Tao, S. Taova, F. Tárkányi, V. V. Varlamov, J. Wang, S.C. Yang, V. Zerkin, Y. Zhuang, Towards a More complete and accurate experimental nuclear reaction data library (EXFOR): International collaboration between nuclear reaction data centres (NRDC), Nucl. Data Sheets. 120 (2014) 272–276. doi:10.1016/j.nds.2014.07.065.

[7] F. Tárkányi, A. Hermanne, B. Király, S. Takács, F. Ditrói, J. Csikai, A. Fenyvesi, M.S. Uddin, M. Hagiwara, M. Baba, T. Ido, Y.N. Shubin, A. V. Ignatyuk, New cross-sections for production of ^{103}Pd; review of charged particle production routes, Appl. Radiat. Isot. 67 (2009) 1574–1581. doi:10.1016/j.apradiso.2009.03.100.

[8] M.U. Khandaker, K. Kim, G. Kim, Production cross sections of short-lived silver radionuclides from ^{nat}Pd(p,xn) nuclear processes, Nucl. Instruments Methods Phys. Res. Sect. B. 274 (2012) 148–153. doi:10.1016/j.nimb.2011.12.022.

[9] F. Tárkányi, F. Ditrói, S. Takács, J. Csikai, A. Hermanne, M.S. Uddin, M. Baba, Activation cross sections of proton induced nuclear reactions on palladium up to 80 MeV, Appl. Radiat. Isot. 114 (2016) 128–144. doi:10.1016/j.apradiso.2016.05.022.

[10] F. Ditrói, F. Tárkányi, S. Takács, A. Hermanne, A. V. Ignatyuk, Measurement of activation cross-section of long-lived products in deuteron induced nuclear reactions on palladium in the 30-50 MeV energy range, Appl. Radiat. Isot. 128 (2017) 297–306. doi:10.1016/j.apradiso.2017.07.049.

[11] N. Ukon, M. Aikawa, Y. Komori, H. Haba, Production cross sections of deuteron-induced reactions on natural palladium for Ag isotopes, Nucl. Instruments Methods Phys. Res. Sect. B. 426 (2018) 13–17. doi:10.1016/j.nimb.2018.04.019.

[12] M. Al-Abyad, F. Tárkányi, F. Ditrói, S. Takács, Excitation function of ^{3}He-particle induced nuclear reactions on natural palladium, Appl. Radiat. Isot. 94 (2014) 191–199. doi:10.1016/j.apradiso.2014.08.002.

[13] A. Hermanne, F. Tárkányi, S. Takács, Y.N. Shubin, Experimental determination of cross section of alpha-induced reactions on ^{nat}Pd, Nucl. Instruments Methods Phys. Res. Sect. B. 229 (2005) 321–332. doi:10.1063/1.1945164.

[14] T. Watanabe, M. Fujimaki, N. Fukunishi, H. Imao, O. Kamigaito, M. Kase, M. Komiyama, N. Sakamoto, K. Suda, M. Wakasugi, K. Yamada, BEAM ENERGY AND LONGITUDINAL BEAM PROFILE MEASUREMENT SYSTEM AT THE RIBF, in: Proc. 5th Int. Part. Accel. Conf. (IPAC 2014), 2014: pp. 3566–3568.

[15] J.F. Ziegler, J.P. Biersack, M.D. Ziegler, SRIM: the Stopping and Range of Ions in Matter, (2008). doi:10.1016/j.nimb.2004.01.208.4.

[16] National Nuclear Data Center, Nuclear structure and decay data on-line library, Nudat 2.7, (2017). http://www.nndc.bnl.gov/nudat2/.

[17] B. Pritychenko, A. Sonzogni, Q-value Calculator (QCalc), (2003). http://www.nndc.bnl.gov/qcalc/.

[18] F. Tárkányi, S. Takács, K. Gul, A. Hermanne, M.G. Mustafa, M. Nortier, P. Obložinský, S.M. Qaim, B. Scholten, Y.N. Shubin, Z. Yousiang, Beam monitor reactions, in: Charg. Part. Cross-Section Database Med. Radioisot. Prod. IAEA-TECDOC-1211, 2001. https://www-nds.iaea.org/medical/monitor_reactions.html.

[19] A.J. Koning, D. Rochman, Modern Nuclear Data Evaluation with the TALYS Code System, Nucl. Data Sheets. 113 (2012) 2841–2934. doi:10.1016/j.nds.2012.11.002.